Author Manuscript

Author Manuscript

Author Manuscript

Author Manuscript

HHS Public Access

Author manuscript

Neurobiol Dis. Author manuscript; available in PMC 2015 May 01.

Published in final edited form as:

Neurobiol Dis. 2011 July ; 43(1): 123–133. doi:10.1016/j.nbd.2011.02.015.

Direct Gene Transfer to the CNS Prevents Emergence of Neurologic Disease in a Murine Model of Mucopolysaccharidosis Type I

Daniel A. Wolf[1], **Andrew W. Lenander**[1], **Zhenhong Nan**[2], **Lalitha R. Belur**[1], **Chester B. Whitley**[1], **Pankaj Gupta**[3], **Walter C. Low**[2], and **R. Scott McIvor**[1]

[1] Gene Therapy Program, Institute of Human Genetics, Department of Genetics, Cell Biology and Development, University of Minnesota, Minneapolis MN 55455 USA

[2] Department of Neurosurgery, University of Minnesota, Minneapolis, MN 55455 USA

[3] Hematology-Oncology Section, Veterans Administration Medical Center, Minneapolis, MN 55417 USA

Abstract

The mucopolysaccharidoses (MPSs) are a group of 11 storage diseases caused by disruptions in glycosaminoglycan (GAG) catabolism, leading to their accumulation in lysosomes. Resultant multisystemic disease is manifested by growth delay, hepatosplenomegaly, skeletal dysplasias, cardiopulmonary obstruction, and, in severe MPS I, II, III, and VII, progressive neurocognitive decline. Some MPSs are treated by allogeneic hematopoietic stem cell transplantation (HSCT) and/or recombinant enzyme replacement therapy (ERT), but effectiveness is limited by central nervous system (CNS) access across the blood-brain barrier. To provide a high level of gene product to the CNS, we tested neonatal intracerebroventricular (ICV) infusion of an adeno-associated virus (AAV) serotype 8 vector transducing the human α-L-iduronidase gene in MPS I mice. Supranormal levels of iduronidase activity in the brain (including 40x normal levels in the hippocampus) were associated with transduction of neurons in motor and limbic areas identifiable by immunofluorescence staining. The treatment prevented accumulation of GAG and GM3 ganglioside storage materials and emergence of neurocognitive dysfunction in a modified Morris water maze test. The results suggest the potential of improved outcome for MPSs and other neurological diseases when a high level of gene expression can be achieved by direct, early administration of vector to the CNS.

© 2011 Elsevier Inc. All rights reserved.

Correspondence should be directed to: R. Scott McIvor (mcivo001@umn.edu). University of Minnesota, Minneapolis MN 55455, Telephone: 612-626-1497, Fax: 612-625-9810.

Publisher's Disclaimer: This is a PDF file of an unedited manuscript that has been accepted for publication. As a service to our customers we are providing this early version of the manuscript. The manuscript will undergo copyediting, typesetting, and review of the resulting proof before it is published in its final citable form. Please note that during the production process errors may be discovered which could affect the content, and all legal disclaimers that apply to the journal pertain.

Author Manuscript Author Manuscript Author Manuscript Author Manuscript

Introduction

The mucopolysaccharidoses (MPSs) are a group of 11 rare, recessive inherited disorders included within the larger family of more than 40 identified lysosomal storage diseases (LSDs). LSDs comprise approximately 14% of all inherited metabolic diseases and affect nearly 1:7,700 births, of which ~30% are MPSs (Meikle et al., 1999; Poorthuis et al., 1999). MPSs are caused by mutations in genes that encode any of the lysosomal hydrolases responsible for the catabolism of GAGs. Genetic deficiency for any of these specific enzymes is associated with growth delay, organomegaly, cardiopulmonary disease, skeletal dysplasias, and obstructive airway disease (Neufeld and Muenzer, 2001). Importantly, individuals with the most severe forms of MPS I, II, III, and VII suffer from severe neurological dysfunction and early death.

Although HSCT and ERT are currently used to treat MPSs, delivery of enzyme to the central nervous system (CNS) remains a major challenge due to the inability of lysosomal enzymes to efficiently cross the blood-brain barrier (Begley et al., 2008; Enns and Huhn, 2008). Early intervention with HSCT has been emphasized for the prevention of cognitive decline in neuropathic MPSs (Boelens et al., 2009; Staba et al., 2004). However, although neurological outcomes for several of the MPSs are improved with donor cell engraftment following HSCT, recipients continue to exhibit below normal IQ and impaired neurocognitive capability (Ziegler and Shapiro, 2007). The aim of this study was to investigate the effects of providing a superior level of enzyme to the brain by direct infusion of an adeno-associated virus (AAV) vector in a murine model of Hurler syndrome (MPS I).

Both AAV2 and AAV5 vectors have been previously used to express lysosomal enzymes in the CNS and to reduce lysosomal GAG storage material following intraparenchymal infusion into mouse models of MPS I (Desmaris et al., 2004), MPS IIIB (Cressant et al., 2004), and MPS VII (Bosch et al., 2000; Frisella et al., 2001; Liu et al., 2007), as well as a dog model of MPS I (Ciron et al., 2006; Ellinwood et al., 2010). In some cases, this has resulted in improved neurobehavior (Cressant et al., 2004; Frisella et al., 2001; Liu et al., 2007). Since AAV8 vectors have been shown to more efficiently transduce neurons within the neonatal mouse brain than either AAV2 or AAV1 vectors (Broekman et al., 2006), we generated an AAV8 vector expressing human α-L-iduronidase (IDUA). This vector was infused into the lateral ventricles of newborn MPS I mice to achieve widespread distribution of the vector through the cerebrospinal fluid and long-term expression of IDUA throughout the brain. Superabundant levels of IDUA activity in limbic areas of the brain were consistent with normalized GAG and GM3 storage materials. Treated mice also exhibited memory and spatial navigation character in a modified Morris water maze that was indistinguishable from unaffected animals. These results demonstrate the potential effectiveness of direct AAV-mediated gene transfer to the brain as a strategy to provide high levels of enzyme activity for prevention of storage accumulation in Hurler syndrome as well as other neuropathic lysosomal storage diseases.

Author Manuscript Author Manuscript Author Manuscript Author Manuscript

Materials and Methods

AAV8-MCI Vector Construction

The *IDUA* expression cassette (mini-CAGS promoter (Ohlfest et al., 2005), human *IDUA* cDNA, bovine growth hormone polyadenylation signal) was excised from plasmid pT2/IDUA//Ub-SB11 (Aronovich et al., 2007) using *Pme*I and *Eco*RV and ligated into the *Sna*BI site of plasmid pSub201 (Samulski et al., 1987). The resulting plasmid, pTR-MCI, contains the *IDUA* expression cassette flanked by AAV2 inverted terminal repeats (Fig 1*A*). This vector was packaged into AAV8 virions at the University of Florida Vector Core by co-transfection of HEK293 cells and purified from cell lysates on an iodixanol step gradient followed by Q Sepharose ion exchange chromatography (Zolotukhin et al., 2002). Vector titer was 4×10^{12} vector genomes/ml.

Animals and ICV Infusions

The *IDUA*$^{-/-}$ mouse strain was provided by Dr. E. Neufeld (Ohmi et al., 2003) and maintained under pathogen-free conditions in AAALAC-accredited facilities. Animal work was reviewed and approved by the Institutional Animal Care and Use Committee of the University of Minnesota. *Idua*$^{-/-}$ pups were generated by breeding homozygous *Idua*$^{-/-}$ animals. All mice were genotyped by PCR as previously described (Hartung et al., 2004). Both male and female four to six-day old *Idua*$^{-/-}$ pups were cryoanesthetized and placed on a stereotactic frame. Five microliters (2×10^{10} vector genomes) of AAV8-MCI was infused into the right-side lateral ventricle (stereotactic coordinates AP 0.0, ML 0.5, DV 1.8 mm from bregma) by hand using a 10 μl Hamilton 701N syringe (Hamilton Chromatography). Briefly, once the syringe was inserted to the designated coordinates, infusion of the AAV vector was begun after a one-minute break. 1 μl of vector was infused per minute for a period of five minutes. After completion of the infusion, the syringe was left in place for two additional minutes before removal of the syringe and suturing of the scalp. The animals were returned to their cages on heating pads for recovery. Following weaning, the mice were housed in groups of 2 to 4 mice of the same sex per cage for the duration of the study.

IDUA Enzyme Assay

At 10 months of age, experimental animals were anesthetized with ketamine/xylazine (100mg ketamine + 10mg xylazine per kg) and transcardially perfused with 70 mL PBS prior to sacrifice. Brains were harvested and microdissected on ice into 12 regions: right and left olfactory bulb, cerebellum, hippocampus, striatum, cortex, and brainstem. The samples were frozen on dry ice and then stored at −80°C. Samples were thawed and homogenized in 1 mL of PBS using a motorized pestle and permeabilized with 0.1% Triton X-100. IDUA activity was determined by fluorometric assay using 4MU-iduronide as the substrate, as previously described (Garcia-Rivera et al., 2007). Activity is expressed in units (percent substrate converted to product per minute) per mg protein as determined by Bradford assay (BioRad).

Author Manuscript Author Manuscript Author Manuscript Author Manuscript

Quantitative PCR

Tissue homogenates were supplemented with 300μl of cell lysis buffer (5 Prime) and with 100μg of proteinase K and incubated with gentle rocking overnight at 55°C. DNA was then isolated from the samples by phenol/chloroform extraction. Reaction mixtures of 25μl contained 0.5μg of DNA, 2X IQ™ SYBR Green Supermix (Bio-Rad) and 200 nM each of forward and reverse primer as previously described (Aronovich et al., 2007). PCR conditions were: 95°C for 2 min, followed by 40 cycles of 95°C for 40 sec, 58°C for 30 sec, and 72°C for 1 min. Mouse glyceraldehyde-3-phosphate dehydrogenase (*Gapdh*) sequence served as an internal control for genomic DNA content and was amplified in a separate reaction. Mouse genomic DNA diluted in water was used as a standard curve for *Gapdh*. The standard curve for IDUA consisted of serial dilutions of DNA isolated from a clone of NIH3T3 cells transduced at low multiplicity with LP1CD retroviral vector (Pan et al., 2000) and assumed to contain 1 viral integrant per cell containing *IDUA*. This DNA was diluted in wild-type C57BL/6 liver DNA to make serial dilutions. All reactions were carried out in duplicate. GAPDH primers used were forward primer: 5′-TGTCTCCTGCGACTTCAACAGC-3′ and reverse primer: 5′-TGTAGGCCATGAGGTCCACCAC-3′. IDUA primers used were forward primer: 5′-AGGAGATACATCGGTACG -3′ and reverse primer: 5′-TGTCAAAGTCGTGGTGGT -3′.

Glycosaminoglycan Assay

Tissue homogenates were clarified by centrifugation for 3 minutes at 13,000 rpm using an Eppendorf tabletop centrifuge model Centrifuge 5415D (Eppendorf) and incubated overnight with proteinase K, DNase1, and RNase as previously described (Garcia-Rivera et al., 2007). GAG concentration was determined using the Blyscan Sulfated Glycosaminoglycan Assay (Accurate Chemical) according to the manufacturer's instructions.

Modified Morris Water Maze

A pool measuring 160 cm in diameter was filled 12 cm deep with water (23°C ± 2°C) mixed with 200 mL of non-toxic white acrylic paint. Three-dimensional, multi-colored visual cues were attached to the walls of the pool according to the cardinal directions (North, South, East, and West) and a platform was submerged 1 cm below the surface of the water in the northwest quadrant of the maze. Age-matched, 5-month old mice were released in the maze facing the southern wall of the pool. The mice were given 90 s to explore the maze and the total time spent swimming before locating the submerged platform was recorded. If a mouse did not reach the platform within 90 s, the animal was guided to the platform and given 30 s to explore. Animals were given 4 trials each day for 10 days, with 12 minutes between each trial. On day 11, a visual platform test was performed in which the submerged platform was moved to the northeast quadrant of the maze and a visual cue was placed directly on the platform, making it visible. The mice were tested using the same protocol, and the time for each mouse to locate the visual platform was recorded.

Author Manuscript Author Manuscript Author Manuscript Author Manuscript

Immunofluorescence

Animals were anesthetized with ketamine/xylazine as above and transcardially perfused with 70mL ice-cold paraformaldehyde (4% w/v in 0.1M PBS) prior to sacrifice. Brains were removed, post-fixed overnight in 4% paraformaldehyde, cryopreserved in sucrose (30% w/v in PBS), frozen on dry ice, and sectioned coronally (30μm thickness) using a freezing microtome. Free-floating sections were washed in PBS and blocked with 10% normal donkey serum/0.3% Triton X-100. Primary antibodies (see legends to Figs. 2, 3, 4, and 5) were added and sections were incubated overnight at 4°C, washed again with PBS, and incubated for 1 hr at room temperature with fluorescently labeled secondary antibodies diluted in PBS. Sections were then washed in PBS, incubated for 10 minutes with DAPI (Invitrogen), mounted on slides, and visualized using a Zeiss Axioplan 2 upright microscope (Zeiss). Primary antibodies were used to stain human IDUA (1:500, R&D Systems), GFAP (1:400, Sigma), NeuN (1:500, Chemicon), and GM3 ganglioside (1:500, Seikagaku). Alexa-conjugated secondary antibodies and dilution factors were as follows: donkey anti-mouse IgG Alexa Fluors 555 and 488 (1:500, Invitrogen), and donkey anti-mouse IgM Alexa Fluor 488 (1:500, Invitrogen).

Statistical Analysis

Data are reported as mean ± s.d. One-way ANOVA with Tukey's post test was used to evaluate statistical differences between groups for the IDUA activity assay, GAG assay, and visual platform behavior assay, with $P < 0.05$ considered significant. For Morris water maze data, the escape latencies for each animal on each day were averaged prior to analyses. Repeated measures two-way ANOVA was used to analyze the data. The *P* values listed signify the variation due to the variable attributed to genotype and/or AAV treatment. All data analysis was performed using Prism 5.0 software (GraphPad Software).

Results

We hypothesized that the emergence of neurological disease might be prevented if sufficient levels of the deficient lysosomal enzyme were expressed after vector-mediated gene transfer to the CNS early in life. To investigate this possibility, we generated an AAV8 vector expressing human IDUA under transcriptional regulation by a strong mini-CAGS promoter (Ohlfest et al., 2005), AAV8-MCI (Fig. 1*A*). This vector produced high levels of IDUA activity following transduction of HEK293 cells in culture (Data not shown). 2×10^{10} vector genomes of AAV8-MCI were infused into the right-hemisphere lateral ventricle of neonatal (P4-P6) IDUA-deficient mice, anticipating that this route of administration would provide widespread distribution and vector-mediated IDUA expression throughout the brain by diffusion through the cerebrospinal fluid.

Intracerebroventricular (ICV) infusion of AAV8-MCI results in supranormal levels of long-term IDUA activity associated with widespread vector transduction

Using a fluorometric assay based on the conversion of 4-methylumbelliferone α-L-iduronide substrate into fluorescent product, IDUA was undetectable in extracts from 10-month-old IDUA-deficient control animals. IDUA levels in extracts from 10-month-old AAV-treated animals exceeded levels detected in wild-type animals for all 12 microdissected regions of

Author Manuscript Author Manuscript Author Manuscript Author Manuscript

the brain (Fig. 1*B*). IDUA activity was highest in brain structures within close proximity to the ventricles. Most notably, activity levels in the hippocampus were ~40-fold higher than those observed in wild-type animals. The striatum, cortex, brainstem, olfactory bulb, and cerebellum exhibited IDUA activity levels that were between 1.5-fold and 15-fold higher than wild-type levels. Although the AAV8-MCI vector was infused unilaterally into the lateral ventricle of the right-hemisphere, we did not observe a significant difference in IDUA activity levels between structures in the left and right hemispheres.

From the same tissue homogenates, total DNA was isolated and the presence of the AAV8-MCI vector was evaluated by quantitative PCR. The vector distribution pattern was consistent with that expected following ICV infusion, with the highest transduction frequencies detected in structures closely juxtaposed to the lateral ventricles (Fig. 1*C*) that also assayed for high levels of IDUA enzyme activity (see above). The greatest level of transduction was detected in both hemispheres of the hippocampus, with transduction frequencies (mean copies/cell: left hemisphere = 42, right hemisphere = 200) similar to those previously reported following direct infusion of AAV vector into the brains of both dogs and macaques (Ciron et al., 2009; Ciron et al., 2006). The level of vector sequences detected in the hippocampus was followed in magnitude by transduction frequencies observed in the cerebral cortex (left hemisphere, mean = 77; right hemisphere, mean = 9.5), striatum (left hemisphere, mean = 7.9; right hemisphere, mean = 1.9), brainstem + thalamus (left hemisphere, mean = 3.2; right hemisphere, mean = 1.9), and olfactory bulb (left hemisphere, mean = 0.48; right hemisphere, mean = 0.75). Relatively low transduction frequencies were detected in the cerebellum (left hemisphere, mean = 0.04; right hemisphere, mean = 0.02) in 4/7 of the animals analyzed and also in the liver (mean = 0.07) of 5/7 animals.

Interestingly, although vector sequences were detected in the cerebellum of only 4/7 treated animals, all of the samples from the cerebellum contained ≥ wild-type levels of IDUA activity. This suggests the possibility of enzymatic cross-correction in this region of the brain. Additionally, although IDUA activity was not detected in the liver of treated animals, we observed the presence of AAV8-MCI vector sequences in 5/7 of the same samples. This suggests a low level of transduction-mediated IDUA activity in the liver that was below the limit of detection using the enzymatic assay, but was nonetheless sufficient to reduce levels of GAG storage material (Fig. 5*A*), similar to observations made in previous reports (Scott et al., 1993; Zheng et al., 2003).

Robust IDUA expression observed within neurons of the limbic system

We further investigated the distribution of IDUA expression at the cellular level by immunofluorescence staining of histologic sections using an antibody to detect human IDUA. In coronal brain sections located at the anterior-posterior coordinates indicated in relation to the bregma (Fig. 2*A*), IDUA staining was most intense in, although not limited to, structures within close proximity to the ventricular system (Figs. 2*B*, *H*, and *N*). Medial to the lateral ventricles, IDUA expression was visualized in the septal nucleus, and in areas CA1, CA2, CA3 and the dentate gyrus of the hippocampus (Figs. 2*F*, *I*, *J*, *L*, and *M*). Dorsal to the lateral ventricles, expression was visualized in the corpus callosum (Data not shown)

Author Manuscript Author Manuscript Author Manuscript Author Manuscript

and much of the cerebral cortex including the cingulate cortex (Fig. 2*D*) region of the limbic cortex. Additionally, the primary motor cortex (Fig. 2*C*), and entorhinal cortex (Fig. 2*K*) (regions involved in motor coordination, and learning and memory, respectively) stained positive for IDUA dorsal to the lateral ventricles. Ventral to the lateral ventricles, positive staining was observed in the caudate putamen (Fig. 2*E*) and nucleus accumbens (Data not shown). The indusium griseum (Fig. 2*G*) and fasciola cinereum (Data not shown) are nuclei lining the 3rd ventricle that stained very intensely with the antibody. Furthermore, Purkinje neurons scattered throughout the cerebellum also stained positive for IDUA, especially in areas immediately dorsal to the 4th ventricle (Figs. 2*N*, *O*). It is likely that the majority of cells that stained positive for IDUA were transduced cells rather than cross-corrected cells, since animals infused in the same manner with an AAV8 vector expressing green fluorescent protein (GFP) displayed a very similar pattern of GFP expression (Figs. 3*A*-*N*) with the exception of immunoreactivity in a different subcellular localization within pyramidal neurons of the hippocampus. Whereas IDUA localized to the soma of the pyramidal cell layer, GFP was observed within the stratum oriens and stratum radiatum layers where the basal and apical dendrites of the pyramidal neurons reside. In summary, IDUA expression was observed at the cellular level in many structures of the limbic system, which are involved in the processes of learning and memory as well as in structures involved in motor function. Robust IDUA expression within these structures may be responsible for the resultant neurophenotype displayed by these animals as described below.

In some cases, the type of cell staining positive for IDUA expression was apparent from the morphologic structure revealed by the staining. For example, Purkinje cells in the cerebellum and pyramidal neurons within the hippocampus were easily identifiable by their characteristic morphology. By co-staining for both IDUA and NeuN (a neuronal cell marker), we verified that much of the IDUA-positive staining observed in the brains of these animals was in neurons (Figs. 4*A*-*D*), as previously reported after infusion of AAV8 vector into the brain (Broekman et al., 2006). However, when co-staining with antibodies to detect both IDUA and GFAP (an astrocytic cell marker), co-localization was not observed (Figs. 4*E*-*H*), demonstrating that most of the IDUA expression was from neuronal rather than astrocytic cells.

Widespread IDUA activity results in normalization of GAG and GM3 ganglioside storage material

The widespread expression and distribution of IDUA had a profound effect on accumulation of storage materials. Total GAG levels were elevated in untreated MPS I mice, but were normalized throughout the brains of AAV8-MCI-treated mice, including the striatum, hippocampus, olfactory bulb, cerebral cortex, cerebellum, brainstem and thalamus, as they were not significantly different from levels observed in unaffected heterozygous or wild-type animals (Fig. 5*A*). Total GAG levels were reduced in the livers of AAV8-MCI-treated mice (perhaps due to enzymatic cross-correction), although they were still significantly higher than those observed in unaffected animals. Secondary accumulation of GM3 ganglioside was apparent in the brains of MPS I animals, as visualized by positive immunofluorescence staining within the white matter as well as in punctate aggregates in cells within the grey matter throughout most of the brain. In contrast, the brains of wild-type

Author Manuscript Author Manuscript Author Manuscript Author Manuscript

and AAV8-MCI treated animals displayed GM3 ganglioside only within white matter (Fig. 5*B*).

AAV8-MCI-treated mice display complete prevention of a neurocognitive deficit in a modified Morris water maze test

At 5 months of age, the experimental animals were subjected to 4 trials of a modified Morris water maze test per day for a duration of 10 days. Unaffected heterozygous littermates exhibited improved performance in this test with repeated trials, requiring an average of 20 seconds to locate the submerged platform at the end of the 10-day testing period. In contrast, untreated MPS I mice displayed a significant deficit in locating the submerged platform (**P = 0.001 by repeated measures two-way ANOVA) (Fig. 6*A*). Remarkably, we observed complete prevention of this neurocognitive impairment in MPS I animals infused with AAV8-MCI at birth, as there was no significant difference observed between these and unaffected heterozygous animals in this test. Wild type animals (not shown) did not perform any better in the water maze than heterozygous animals. On day 11 of the testing period, the submerged platform was moved to the northeast quadrant of the maze and a visual cue was placed directly on the platform. MPS I mice were able to locate the visible platform much faster than the submerged platform and did not perform significantly different than unaffected animals (Fig. 6*B*). This demonstrates that the observed phenotype was neurocognitive in nature and not the result of impaired vision or of musculoskeletal or cardiopulmonary dysfunction in the MPS I animals.

Discussion

We observed extraordinarily high levels of vector transduction and long-term IDUA activity throughout the brains of animals infused ICV with AAV8-MCI at birth, consistent with prevention of accumulated GAG and GM3 ganglioside storage materials. The majority of the IDUA expression was in neurons of the hippocampus and limbic areas as well as in Purkinje cells of the cerebellum. Although a portion of IDUA is able to find its way into the extracellular space (Vladutiu and Rattazzi, 1979), most of the IDUA observed by immunofluorescence likely came from transduced cells rather than metabolically cross-corrected cells, since the brains of MPS I neonates transduced with AAV8-GFP displayed a similar pattern of immunostaining.

Gene therapy has long been considered to be a potentially effective approach for the lysosomal storage diseases, particularly the MPSs. The effectiveness of HSCT and ERT is based upon the phenomenon of metabolic cross-correction, whereby enzyme released from normal cells or infused into the circulation can be taken up by host cells through interaction with mannose 6-phosphate receptors and trafficked to lysosomes, where it participates in lysosomal metabolism and degradation of accumulated GAG (Fratantoni et al., 1968; Hille-Rehfeld, 1995; Rome et al., 1979; Vladutiu and Rattazzi, 1979). This concept is particularly applicable to gene therapy, whereby cells can be genetically engineered to express high levels of enzyme for metabolic cross correction. For many of the MPSs, milder non-neuropathic forms of disease are observed in patients that retain only a small percentage of normal enzymatic activity (Bunge et al., 1998; Weber et al., 1999). This argues that a high

Author Manuscript Author Manuscript Author Manuscript Author Manuscript

level of overall enzyme activity may not be required to prevent the pathologic accumulation of storage materials in the brain. This is consistent with the benefit to the CNS observed in MPS I patients following HSCT, likely the result of a small amount of IDUA enzyme expressed by donor-derived microglia in the brain (Guffon et al., 1998; Peters et al., 1996; Peters et al., 1998). A goal of gene therapy for MPSs is to achieve a higher level of enzyme in the brain that will more effectively prevent accumulation of neuropathic storage materials.

In this regard, animal models of the MPSs have provided a formative testing ground for evaluating different gene transfer and expression strategies targeting peripheral and neurologic manifestations of storage disease. Building on the concept of HSCT, *ex vivo* transduction of autologous hematopoietic stem cells, first using gammaretroviral vectors and then more recently using lentiviral vectors, has been explored in both murine and canine models of MPS disease (Lutzko et al., 1999; Marechal et al., 1993; Ohashi et al., 2000; Traas et al., 2007; Visigalli et al., 2010; Zheng et al., 2003). Direct intravenous administration of retroviral, lentiviral and AAV vectors has also shown efficacy in several MPS animal models (Cardone et al., 2006; Chung et al., 2007; Daly et al., 1999; Di Domenico et al., 2005; Hartung et al., 2004; Kobayashi et al., 2005; Ma et al., 2007; Traas et al., 2007). The potential effectiveness of these approaches in preventing neurodegeneration is presumably dependent upon either enzyme expression in or enzyme delivery to the CNS, thus requiring (i) vector trafficking to the CNS after intravenous administration; (ii) penetration of the CNS by transduced hematopoietic cells after *ex vivo* transduction of hematopoietic stem cells; or (iii) penetration of the CNS by enzyme expressed in a peripheral organ such as the liver after intravenous administration of vector.

While examples of neurologic efficacy have been reported after intravenous vector delivery, direct administration of vector to the CNS ensures gene delivery and enzyme expression in CNS tissues. This approach has been used to demonstrate prevention of neurodegeneration in MPS VII mice after intracranial infusion of AAV2, 4, and 5 vectors transducing the β-glucuronidase gene (Frisella et al., 2001; Liu et al., 2007; Liu et al., 2005). For MPS I, correction of neuropathology in enzyme-deficient mice has been achieved following intraparenchymal infusion of AAV2 or AAV5 vectors encoding *IDUA* (Desmaris et al., 2004). AAV5-mediated *IDUA* gene transfer has also been reported in the canine MPS I model, demonstrating widespread distribution and correction of GAG accumulation up to 8 months after infusion (Ciron et al., 2006; Ellinwood et al., 2010) In this paper, we demonstrate the effectiveness of AAV8 pseudotyped vector in achieving high-level IDUA expression in the brain after intracerebroventricular infusion into neonatal MPS I mice. We furthermore demonstrate that this level of expression completely prevented neurocognitive decline in these animals, a clear benefit from direct vector administration to the CNS.

Granular storage material within lysosomes of neurons and glia, as well as characteristic lamellar zebra body formation within cerebral neurons, have been described in MPS I animals (Shull et al., 1987). Although seemingly unrelated to GAGs, accumulation of GM2 and GM3 gangliosides has additionally been observed in the brains of MPS patients (Jones et al., 1997) and animals (Liour et al., 2001; McGlynn et al., 2004; Ohmi et al., 2003; Walkley et al., 2005). It is not well understood how the accumulation of these molecules leads to neurological disease in the MPSs, although aberrancy of several processes has been

Author Manuscript Author Manuscript Author Manuscript Author Manuscript

implicated. GM2 and GM3 accumulation in affected neurons is associated with ectopic dendritogenesis and altered synaptic plasticity in humans (Walkley et al., 2000). Additionally, accumulation of storage materials has been proposed to disrupt cell signaling, induce apoptosis, and cause oxidative damage (Pan et al., 2005; Villani et al., 2007). It is likely that neurodegenerative processes related to storage material accumulation were interrupted and/or prevented by AAV8-MCI infusion in MPS I mice, since GAG accumulation was normalized and GM3 ganglioside accumulation was not observed.

We presume that the complete prevention of a deficit in the modified MWM in our treated mice is the result of preserved neural circuitry related to learning and memory, which is damaged in untreated animals. Importantly, many structures of the brain where IDUA expression was visualized by immunofluorescence are intimately involved in the cognitive processes required for learning and memory in the MWM. For instance, hippocampal place cells are thought to be primarily required for spatial memory and navigation skills in hidden platform learning in the MWM test (Poucet et al., 2000). Gerbils with ischemic injury that selectively destroys CA1 hippocampal pyramidal cells exhibit deficits in spatial navigation performance in the MWM (Onifer and Low, 1990). Rats with quinolinic acid induced lesions in the striatum display a deficit in MWM hidden platform acquisition and spend much of their time swimming along the walls of the maze (thigmotaxis), as observed in our untreated MPS I control group (Block et al., 1993). Additionally, rats with lesions of the medial septal nucleus or the cingulate cortex and mice with cerebellar damage all have impaired MWM performance (Brandner and Schenk, 1998; Lalonde, 1994; Warburton et al., 1998). IDUA expression was visualized in neurons within all of these areas of the brain, suggesting that this pattern of expression may be in part responsible for the complete prevention of a neurocognitive deficit in the MWM.

While neurological outcomes for several of the neuropathogenic MPSs are improved with engraftment following HSCT, recipients nonetheless continue to exhibit below normal IQ and impaired neurocognitive capability (Ziegler and Shapiro, 2007). Our results predict that AAV-mediated IDUA gene delivery to the CNS, by way of ICV infusion, will provide a sustained, high level of enzyme expression that vastly exceeds the amount reasonably attainable by ERT or HSCT (Vogler et al., 2005; Zheng et al., 2003), with improved neurological outcome anticipated.

Although the current study focused on the use of AAV8 as an effective vector for gene transfer into neonatal mice (Broekman et al., 2006), further preclinical development must include consideration of other serotypes, such as AAV9 (Foust et al., 2009) and AAVrh.10, which has been shown to outperform AAV8 in a rat model of the lysosomal storage disorder Batten's disease (Sondhi et al., 2007) and is currently in clinical testing. Numerous AAV serotypes (1 – 6 and 8) have been tested for gene transfer in the brain of non-human primates (Ciron et al., 2009; Dodiya et al., 2010; Hadaczek et al., 2009; Markakis et al., 2010), although intracerebroventricular infusion has not been reported.

Despite the overall success of the current study, there are several limitations in its interpretation when considering the treatment of MPS children. Human IDUA is known to be highly immunogenic, and has been shown to elicit both humoral and cytotoxic T

Author Manuscript Author Manuscript Author Manuscript Author Manuscript

lymphocyte responses in adult MPS I mice, newborn cats, and dogs (Di Domenico et al., 2006; Di Domenico et al., 2005; Lutzko et al., 1999; Ma et al., 2007; Ponder et al., 2006; Shull et al., 1996). Newborn mice are immunologically naïve (Adkins et al., 2004; Landers et al., 2005; Ponder, 2007; Schelonka and Infante, 1998; West, 2002), so it is possible that our AAV-treated animals were immunotolerized by the expression of IDUA soon after birth, before development of the immune system as we have previously observed (Hartung et al., 2004). Also, a significant challenge will be the application of ICV infusion of AAV to achieve gene transfer in the human brain, which is several thousand-fold larger than the neonatal mouse brain and in which the effectiveness of the procedure will be further limited by diffusion of the vector into deep brain tissues. Nonetheless, results of this study strongly support the adoption of CNS-directed, AAV-mediated gene therapy as a supplement to ERT and HSCT for the treatment of MPSs (Tolar et al., 2008), to provide effective treatment for both peripheral and CNS manifestations in patients with severe lysosomal storage disease. Although there are significant challenges to be faced in scale-up, route of administration, and assessment of procedural safety, the benefits of high-level neonatal AAV-mediated transduction in the CNS are potentially applicable to the treatment of a broad range of neurological disorders.

Acknowledgments

We thank Dr. P. Hackett and Dr. E. Aronovich for helpful advice on quantitative PCR reactions, B. Koniar for animal care, and S. Sandberg and R. Cooksley for animal genotyping. We thank the staff at the Powell Gene Therapy Vector Core for preparation and titering of AAV vector used in this study. This work was supported by NIH grant P01 HD032652 (CBW, RSM) and training grant T32 DA022616-01 (DAW).

References

Adkins, B., et al. Neonatal adaptive immunity comes of age. England: 2004.

Aronovich EL, et al. Prolonged expression of a lysosomal enzyme in mouse liver after Sleeping Beauty transposon-mediated gene delivery: implications for non-viral gene therapy of mucopolysaccharidoses. J Gene Med. 2007; 9:403–15. [PubMed: 17407189]

Begley DJ, et al. Lysosomal storage diseases and the blood-brain barrier. Curr Pharm Des. 2008; 14:1566–80. [PubMed: 18673198]

Block F, et al. Quinolinic acid lesion of the striatum induces impairment in spatial learning and motor performance in rats. Neurosci Lett. 1993; 149:126–8. [PubMed: 8474683]

Boelens JJ, et al. Risk factor analysis of outcomes after unrelated cord blood transplantation in patients with hurler syndrome. Biol Blood Marrow Transplant. 2009; 15:618–25. [PubMed: 19361754]

Bosch A, et al. Long-term and significant correction of brain lesions in adult mucopolysaccharidosis type VII mice using recombinant AAV vectors. Mol Ther. 2000; 1:63–70. [PubMed: 10933913]

Brandner C, Schenk F. Septal lesions impair the acquisition of a cued place navigation task: attentional or memory deficit? Neurobiol Learn Mem. 1998; 69:106–25. [PubMed: 9619991]

Broekman ML, et al. Adeno-associated virus vectors serotyped with AAV8 capsid are more efficient than AAV-1 or -2 serotypes for widespread gene delivery to the neonatal mouse brain. Neuroscience. 2006; 138:501–10. [PubMed: 16414198]

Bunge S, et al. Genotype-phenotype correlations in mucopolysaccharidosis type I using enzyme kinetics, immunoquantification and in vitro turnover studies. Biochim Biophys Acta. 1998; 1407:249–56. [PubMed: 9748610]

Burger C, et al. Recombinant AAV viral vectors pseudotyped with viral capsids from serotypes 1, 2, and 5 display differential efficiency and cell tropism after delivery to different regions of the central nervous system. Mol Ther. 2004; 10:302–17. [PubMed: 15294177]

Author Manuscript Author Manuscript Author Manuscript Author Manuscript

Cardone M, et al. Correction of Hunter syndrome in the MPSII mouse model by AAV2/8-mediated gene delivery. Human Molecular Genetics. 2006; 15:1225–36. [PubMed: 16505002]

Chung S, et al. Effect of neonatal administration of a retroviral vector expressing alpha-L-iduronidase upon lysosomal storage in brain and other organs in mucopolysaccharidosis I mice. Mol Genet Metab. 2007; 90:181–92. [PubMed: 16979922]

Ciron C, et al. Human alpha-iduronidase gene transfer mediated by adeno-associated virus types 1, 2, and 5 in the brain of nonhuman primates: vector diffusion and biodistribution. Hum Gene Ther. 2009; 20:350–60. [PubMed: 19272011]

Ciron C, et al. Gene therapy of the brain in the dog model of Hurler's syndrome. Ann Neurol. 2006; 60:204–13. [PubMed: 16718701]

Cressant A, et al. Improved behavior and neuropathology in the mouse model of Sanfilippo type IIIB disease after adeno-associated virus-mediated gene transfer in the striatum. J Neurosci. 2004; 24:10229–39. [PubMed: 15537895]

Daly TM, et al. Neonatal gene transfer leads to widespread correction of pathology in a murine model of lysosomal storage disease. Proc Natl Acad Sci U S A. 1999; 96:2296–300. [PubMed: 10051635]

Desmaris N, et al. Prevention of neuropathology in the mouse model of Hurler syndrome. Ann Neurol. 2004; 56:68–76. [PubMed: 15236403]

Di Domenico C, et al. Limited transgene immune response and long-term expression of human alpha-L-iduronidase in young adult mice with mucopolysaccharidosis type I by liver-directed gene therapy. Hum Gene Ther. 2006; 17:1112–21. [PubMed: 17044753]

Di Domenico C, et al. Gene therapy for a mucopolysaccharidosis type I murine model with lentiviral-IDUA vector. Hum Gene Ther. 2005; 16:81–90. [PubMed: 15703491]

Dodiya HB, et al. Differential transduction following basal ganglia administration of distinct pseudotyped AAV capsid serotypes in nonhuman primates. Mol Ther. 2010; 18:579–87. [PubMed: 19773746]

Ellinwood NM, et al. Safe, efficient, and reproducible gene therapy of the brain in the dog models of Sanfilippo and hurler syndromes. Mol Ther. 2010; 19:251–9. [PubMed: 21139569]

Enns GM, Huhn SL. Central nervous system therapy for lysosomal storage disorders. Neurosurg Focus. 2008; 24:E12. [PubMed: 18341388]

Foust KD, et al. Intravascular AAV9 preferentially targets neonatal neurons and adult astrocytes. Nat Biotechnol. 2009; 27:59–65. [PubMed: 19098898]

Fratantoni JC, et al. Hurler and Hunter syndromes: mutual correction of the defect in cultured fibroblasts. Science. 1968; 162:570–2. [PubMed: 4236721]

Frisella WA, et al. Intracranial injection of recombinant adeno-associated virus improves cognitive function in a murine model of mucopolysaccharidosis type VII. Mol Ther. 2001; 3:351–8. [PubMed: 11273777]

Garcia-Rivera MF, et al. Characterization of an immunodeficient mouse model of mucopolysaccharidosis type I suitable for preclinical testing of human stem cell and gene therapy. Brain Res Bull. 2007; 74:429–38. [PubMed: 17920451]

Guffon N, et al. Follow-up of nine patients with Hurler syndrome after bone marrow transplantation. J Pediatr. 1998; 133:119–25. [PubMed: 9672523]

Hadaczek P, et al. Transduction of nonhuman primate brain with adeno-associated virus serotype 1: vector trafficking and immune response. Hum Gene Ther. 2009; 20:225–37. [PubMed: 19292604]

Hartung SD, et al. Correction of metabolic, craniofacial, and neurologic abnormalities in MPS I mice treated at birth with adeno-associated virus vector transducing the human alpha-L-iduronidase gene. Mol Ther. 2004; 9:866–75. [PubMed: 15194053]

Hille-Rehfeld A. Mannose 6-phosphate receptors in sorting and transport of lysosomal enzymes. Biochim Biophys Acta. 1995; 1241:177–94. [PubMed: 7640295]

Jones MZ, et al. Human mucopolysaccharidosis IIID: clinical, biochemical, morphological and immunohistochemical characteristics. J Neuropathol Exp Neurol. 1997; 56:1158–67. [PubMed: 9329460]

Kobayashi H, et al. Neonatal gene therapy of MPS I mice by intravenous injection of a lentiviral vector. Mol Ther. 2005; 11:776–89. [PubMed: 15851016]

Author Manuscript Author Manuscript Author Manuscript Author Manuscript

Lalonde R. Cerebellar contributions to instrumental learning. Neurosci Biobehav Rev. 1994; 18:161–70. [PubMed: 8058211]

Landers, CD., et al., editors. The role of B cells and accessory cells in the neonatal response to TI-2 antigens. United States; 2005.

Liour SS, et al. Metabolic studies of glycosphingolipid accumulation in mucopolysaccharidosis IIID. Mol Genet Metab. 2001; 72:239–47. [PubMed: 11243730]

Liu G, et al. Adeno-associated virus type 5 reduces learning deficits and restores glutamate receptor subunit levels in MPS VII mice CNS. Mol Ther. 2007; 15:242–7. [PubMed: 17235300]

Liu G, et al. Functional correction of CNS phenotypes in a lysosomal storage disease model using adeno-associated virus type 4 vectors. J Neurosci. 2005; 25:9321–7. [PubMed: 16221840]

Lutzko C, et al. Genetically corrected autologous stem cells engraft, but host immune responses limit their utility in canine alpha-L-iduronidase deficiency. Blood. 1999; 93:1895–905. [PubMed: 10068662]

Ma X, et al. Improvements in mucopolysaccharidosis I mice after adult retroviral vector-mediated gene therapy with immunomodulation. Mol Ther. 2007; 15:889–902. [PubMed: 17311010]

Marechal V, et al. Disappearance of lysosomal storage in spleen and liver of mucopolysaccharidosis VII mice after transplantation of genetically modified bone marrow cells. Blood. 1993; 82:1358–65. [PubMed: 8353294]

Markakis EA, et al. Comparative transduction efficiency of AAV vector serotypes 1–6 in the substantia nigra and striatum of the primate brain. Mol Ther. 2010; 18:588–93. [PubMed: 20010918]

McGlynn R, et al. Differential subcellular localization of cholesterol, gangliosides, and glycosaminoglycans in murine models of mucopolysaccharide storage disorders. J Comp Neurol. 2004; 480:415–26. [PubMed: 15558784]

Meikle PJ, et al. Prevalence of lysosomal storage disorders. Jama. 1999; 281:249–54. [PubMed: 9918480]

Neufeld, EF.; Muenzer, J. The mucopolysaccharidoses. In: Scriver, ALBCR.; Sly, WS., et al., editors. The metabolic and molecular bases of inherited disease. McGraw Hill; New York: 2001. p. 3421-3452.

Ohashi T, et al. Reduction of lysosomal storage in murine mucopolysaccharidosis type VII by transplantation of normal and genetically modified macrophages. Blood. 2000; 95:3631–3. [PubMed: 10828055]

Ohlfest JR, et al. Phenotypic correction and long-term expression of factor VIII in hemophilic mice by immunotolerization and nonviral gene transfer using the Sleeping Beauty transposon system. Blood. 2005; 105:2691–8. [PubMed: 15576475]

Ohmi K, et al. Activated microglia in cortex of mouse models of mucopolysaccharidoses I and IIIB. Proc Natl Acad Sci U S A. 2003; 100:1902–7. [PubMed: 12576554]

Onifer SM, Low WC. Spatial memory deficit resulting from ischemia-induced damage to the hippocampus is ameliorated by intra-hippocampal transplants of fetal hippocampal neurons. Prog Brain Res. 1990; 82:359–66. [PubMed: 2290949]

Pan C, et al. Functional abnormalities of heparan sulfate in mucopolysaccharidosis-I are associated with defective biologic activity of FGF-2 on human multipotent progenitor cells. Blood. 2005; 106:1956–64. [PubMed: 15947088]

Pan D, et al. Retroviral vector design studies toward hematopoietic stem cell gene therapy for mucopolysaccharidosis type I. Gene Ther. 2000; 7:1875–83. [PubMed: 11110421]

Peters C, et al. Outcome of unrelated donor bone marrow transplantation in 40 children with Hurler syndrome. Blood. 1996; 87:4894–902. [PubMed: 8639864]

Peters C, et al. Hurler syndrome: II. Outcome of HLA-genotypically identical sibling and HLA-haploidentical related donor bone marrow transplantation in fifty-four children. The Storage Disease Collaborative Study Group. Blood. 1998; 91:2601–8. [PubMed: 9516162]

Ponder KP. Immunology of neonatal gene transfer. Curr Gene Ther. 2007; 7:403–10. [PubMed: 17979686]

Author Manuscript Author Manuscript Author Manuscript Author Manuscript

Ponder KP, et al. Mucopolysaccharidosis I cats mount a cytotoxic T lymphocyte response after neonatal gene therapy that can be blocked with CTLA4-Ig. Mol Ther. 2006; 14:5–13. [PubMed: 16698321]

Poorthuis BJ, et al. The frequency of lysosomal storage diseases in The Netherlands. Hum Genet. 1999; 105:151–6. [PubMed: 10480370]

Poucet B, et al. Sensory and memory properties of hippocampal place cells. Rev Neurosci. 2000; 11:95–111. [PubMed: 10718148]

Rome LH, et al. Direct demonstration of binding of a lysosomal enzyme, alpha-L-iduronidase, to receptors on cultured fibroblasts. Proc Natl Acad Sci U S A. 1979; 76:2331–4. [PubMed: 287076]

Samulski RJ, et al. A recombinant plasmid from which an infectious adeno-associated virus genome can be excised in vitro and its use to study viral replication. J Virol. 1987; 61:3096–101. [PubMed: 3041032]

Schelonka RL, Infante AJ. Neonatal immunology. Seminars in perinatology. 1998; 22:2–14. [PubMed: 9523395]

Scott HS, et al. Identification of mutations in the alpha-L-iduronidase gene (IDUA) that cause Hurler and Scheie syndromes. Am J Hum Genet. 1993; 53:973–86. [PubMed: 8213840]

Shull R, et al. Humoral immune response limits gene therapy in canine MPS I. Blood. 1996; 88:377–9. [PubMed: 8704199]

Shull RM, et al. Bone marrow transplantation in canine mucopolysaccharidosis I. Effects within the central nervous system. J Clin Invest. 1987; 79:435–43. [PubMed: 3100576]

Sondhi D, et al. Enhanced survival of the LINCL mouse following CLN2 gene transfer using the rh.10 rhesus macaque-derived adeno-associated virus vector. Mol Ther. 2007; 15:481–91. [PubMed: 17180118]

Staba SL, et al. Cord-blood transplants from unrelated donors in patients with Hurler's syndrome. N Engl J Med. 2004; 350:1960–9. [PubMed: 15128896]

Tolar J, et al. Combination of enzyme replacement and hematopoietic stem cell transplantation as therapy for Hurler syndrome. Bone Marrow Transplant. 2008; 41:531–5. [PubMed: 18037941]

Traas AM, et al. Correction of clinical manifestations of canine mucopolysaccharidosis I with neonatal retroviral vector gene therapy. Mol Ther. 2007; 15:1423–31. [PubMed: 17519893]

Villani GR, et al. Cytokines, neurotrophins, and oxidative stress in brain disease from mucopolysaccharidosis IIIB. J Neurosci Res. 2007; 85:612–22. [PubMed: 17139681]

Visigalli I, et al. Gene therapy augments the efficacy of hematopoietic cell transplantation and fully corrects Mucopolysaccharidosis type I phenotype in the mouse model. Blood. 2010

Vladutiu GD, Rattazzi MC. Excretion-reuptake route of beta-hexosaminidase in normal and I-cell disease cultured fibroblasts. J Clin Invest. 1979; 63:595–601. [PubMed: 438323]

Vogler C, et al. Overcoming the blood-brain barrier with high-dose enzyme replacement therapy in murine mucopolysaccharidosis VII. Proc Natl Acad Sci U S A. 2005; 102:14777–82. [PubMed: 16162667]

Walkley SU, et al. Abnormal neuronal metabolism and storage in mucopolysaccharidosis type VI (Maroteaux-Lamy) disease. Neuropathol Appl Neurobiol. 2005; 31:536–44. [PubMed: 16150124]

Walkley SU, et al. Gangliosides as modulators of dendritogenesis in normal and storage disease-affected pyramidal neurons. Cereb Cortex. 2000; 10:1028–37. [PubMed: 11007553]

Warburton EC, et al. Comparing the effects of selective cingulate cortex lesions and cingulum bundle lesions on water maze performance by rats. Eur J Neurosci. 1998; 10:622–34. [PubMed: 9749724]

Weber B, et al. Sanfilippo type B syndrome (mucopolysaccharidosis III B): allelic heterogeneity corresponds to the wide spectrum of clinical phenotypes. Eur J Hum Genet. 1999; 7:34–44. [PubMed: 10094189]

West LJ. Defining critical windows in the development of the human immune system. Human & experimental toxicology. 2002; 21:499–505. [PubMed: 12458907]

Zheng Y, et al. Treatment of the mouse model of mucopolysaccharidosis I with retrovirally transduced bone marrow. Mol Genet Metab. 2003; 79:233–44. [PubMed: 12948739]

Author Manuscript Author Manuscript Author Manuscript Author Manuscript

Ziegler, R.; Shapiro, E. Metabolic and neurodegenerative diseases across the life span. In: Donder, SHJ., editor. Principles and Practice of Lifespan Developmental Neuropsychology. Cambridge University Press; 2007. p. 427-448.

Zolotukhin S, et al. Production and purification of serotype 1, 2, and 5 recombinant adeno-associated viral vectors. Methods. 2002; 28:158–67. [PubMed: 12413414]

Author Manuscript Author Manuscript Author Manuscript Author Manuscript

Research Highlights

- Intracerebroventricular infusion of an AAV8 vector into neonates results in long-term, widespread α-L-iduronidase expression.
- Cells expressing IDUA include neurons within regions of the limbic system and Purkinje cells of the cerebellum.
- AAV treatment results in normalization of lysosomal storage materials in all brain regions.
- Treated animals display complete prevention of a neurocognitive deficit in a Morris water maze test.

Author Manuscript Author Manuscript Author Manuscript Author Manuscript

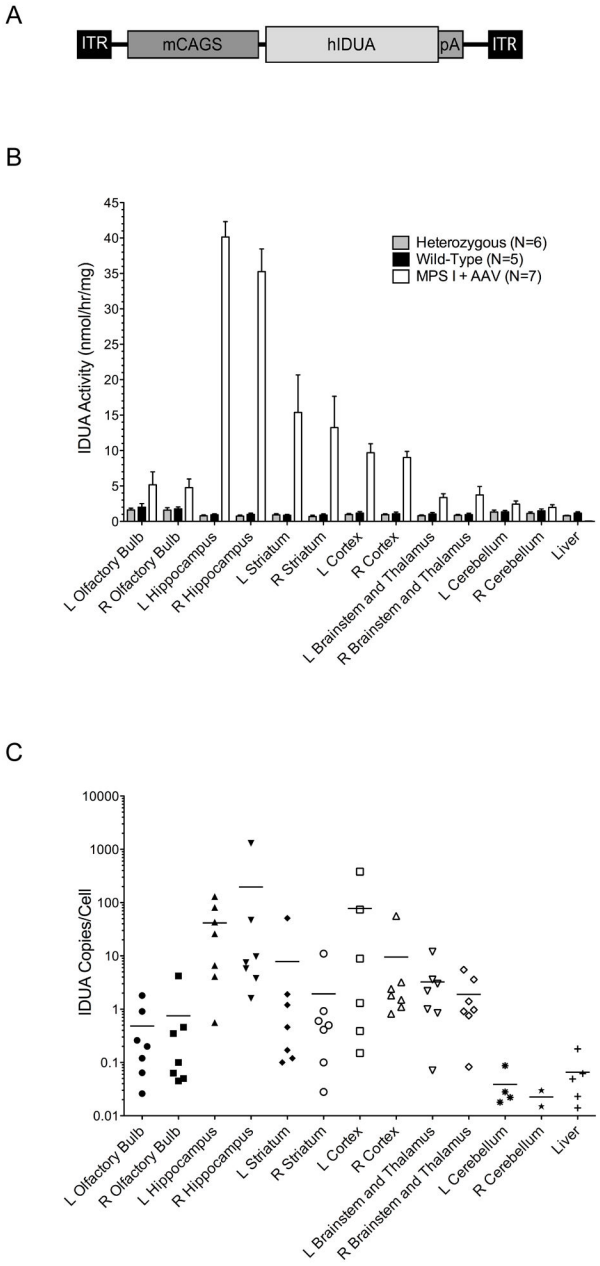

Figure 1.

ICV infusion of AAV8-MCI into neonatal mice results in widespread AAV2/8-MCI transduction associated with long-term high-level expression of IDUA throughout the brain. ***A***, Depiction of the therapeutic AAV construct. AAV serotype 2 inverted terminal repeat (ITR) sequences flank the human *IDUA* cDNA regulated by a mini-CAGS (mCAGS) promoter. This construct was packaged using AAV serotype 8 capsids to produce AAV8-MCI. ***B***, IDUA activity levels in brain tissues at 10 months of age. Brain tissues were microdissected from wild-type, heterozygous, and MPS I animals treated at birth by ICV infusion with AAV8-MCI and assayed for IDUA activity (mean +/− S.D.). Enzyme activity levels in treated mice were well above those detected in the brains of wild-type animals in

Author Manuscript Author Manuscript Author Manuscript Author Manuscript

all samples studied. The activity levels follow a gradient pattern with the highest levels of activity present within brain regions in close proximity to the lateral ventricles. IDUA activity was undetectable in extracts prepared from untreated MPS I animals. ***C***, IDUA vector sequences (copies per genome equivalent) detected in brain tissue samples by quantitative PCR. The transduction pattern displayed by AAV8-MCI follows a pattern of distribution throughout the brain similar to that displayed by the enzyme activity data presented in *B*. Bar = mean.

Author Manuscript Author Manuscript Author Manuscript Author Manuscript

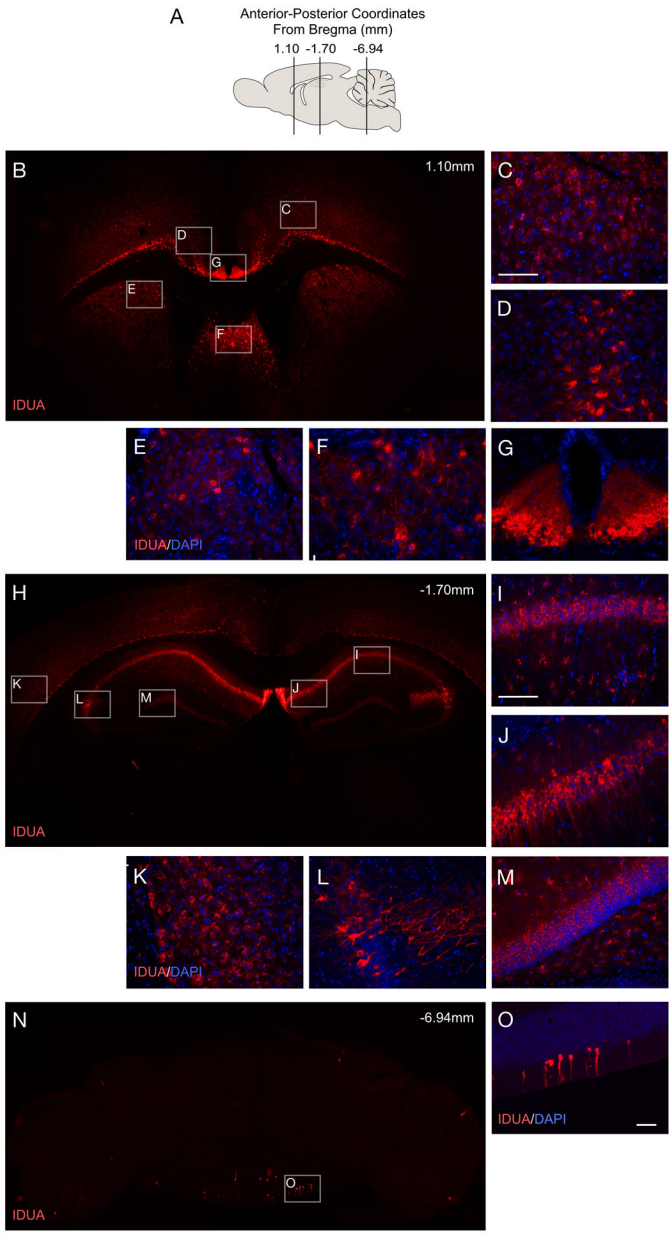

Figure 2.

Immunofluorescence staining with an anti-IDUA antibody reveals widespread IDUA expression, mainly in neuronal cells within areas of the limbic system. Coronal brain slices taken at the displayed coordinates from the bregma (***A***) were stained with an anti-human IDUA antibody. Low magnification images reveal widespread distribution of IDUA expression (red) (***B***, ***H***, ***M***). Higher-power magnification of specific regions within the section reveals IDUA expression (IDUA (red) and DAPI (blue)) in multiple areas of the limbic system including the cingulate cortex (***D***), septal nucleus (***F***), indusium griseum (***G***), hippocampus (CA1 (***I***), CA2 (***J***), CA3 (***L***), and dentate gyrus (***M***)), entorhinal cortex (***K***), and basal ganglia (caudate putamen (***E***)). Additionally, regions of the brain important for motor function displayed robust IDUA expression, including the primary motor cortex (***C***)

and Purkinje cells lining the 4th ventricle in the cerebellum (***O***). Representative scale bars in panels (***C***), (***I***), and (***O***) are 100μm in length.

Author Manuscript Author Manuscript Author Manuscript Author Manuscript

Author Manuscript Author Manuscript Author Manuscript Author Manuscript

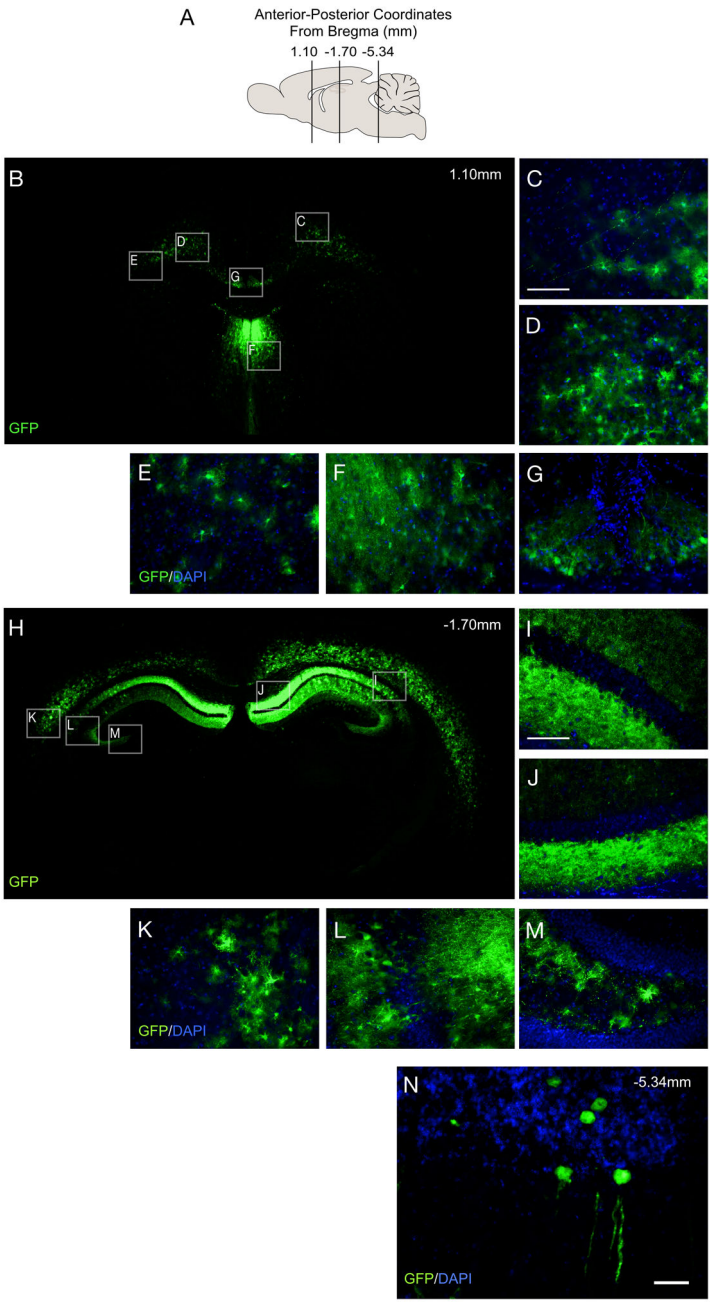

Figure 3.

ICV infusion of an AAV8-GFP vector results in a similar transgene expression pattern as observed following ICV infusion of AAV8-MCI at birth. 2×10^{10} vector genomes of AAV8-TRUF11 (Burger et al., 2004) was infused into the right side lateral ventricle of *IDUA*$^{-/-}$ neonates as described in the methods for AAV8-MCI. Coronal brain sections taken at the displayed anterior-posterior coordinates from the bregma (***A***) were stained with an anti-GFP antibody. Low power magnification images reveal widespread distribution of GFP expression (green) (***B***, ***H***). Higher-power magnification of specific regions reveals GFP expression (GFP (green) and DAPI (blue)) in multiple areas of the limbic system including

Author Manuscript Author Manuscript Author Manuscript Author Manuscript

the cingulate cortex (***D***), septal nucleus (***F***), indusium griseum (***G***), hippocampus, (CA1 (***I***), CA2 (***J***), CA3 (***L***), and dentate gyrus (***M***)), entorhinal cortex (***K***), and basal ganglia (caudate putamen (***E***)). Additionally, regions of the brain important for motor function displayed robust GFP expression, including the primary motor cortex (***C***) and Purkinje cells lining the 4th ventricle in the cerebellum (***O***). This pattern of expression is comparable to that observed after ICV infusion of AAV8-MCI. Scale bars are 100μm in length.

Author Manuscript Author Manuscript Author Manuscript Author Manuscript

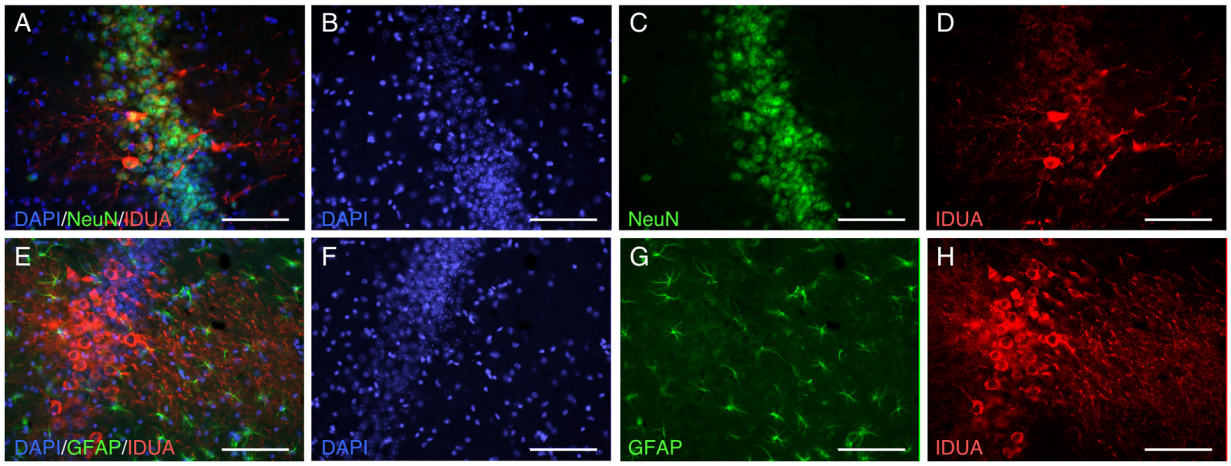

Figure 4.

IDUA is expressed primarily in neurons rather than in astrocytes. Cells expressing IDUA (red) displayed a strong co-localization with NeuN (green) resulting in yellow co-staining within pyramidal neurons of area CA3 of the hippocampus (***A-D***). However, in the same region of the brain, IDUA (red) did not co-localize with the astrocytic marker GFAP (green) (*E-H*). Scale bars are 100μm in length.

Author Manuscript Author Manuscript Author Manuscript Author Manuscript

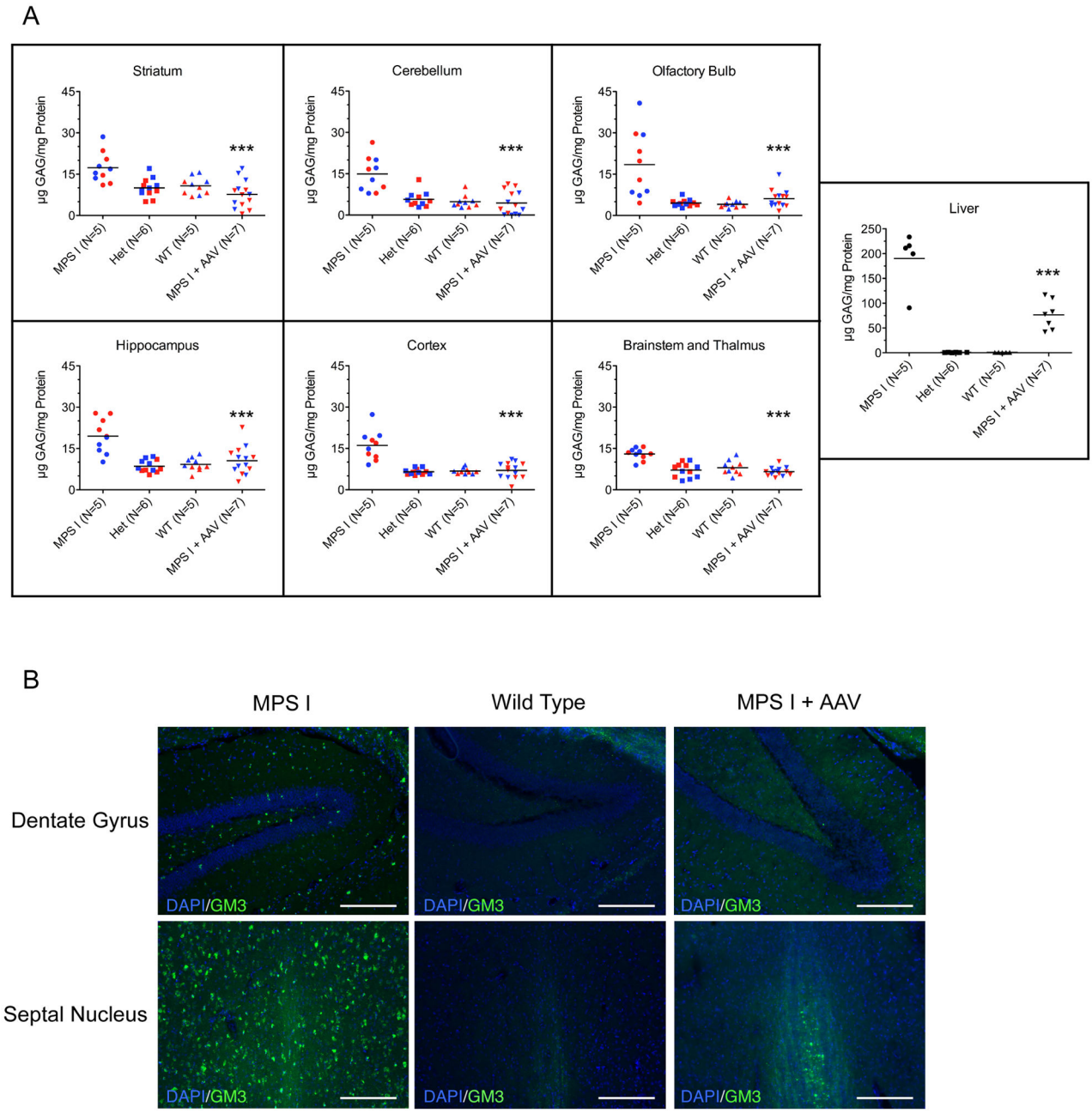

Figure 5.

ICV infusion of AAV8-MCI into neonates normalized pathogenic storage material to levels of unaffected animals. ***A***, Total GAG levels in the striatum, olfactory bulb, cerebellum, hippocampus, cortex, striatum, brainstem and thalamus, and livers of wild-type, *IDUA* heterozygous, MPS 1, and AAV8-MCI treated MPS I mice. Data points represent brain samples microdissected from the left (red) and right (blue) hemispheres, respectively. Values are compared to respective values in untreated MPS I animals (horizontal bar: mean; ***$P < 0.001$). ***B***, Punctate GM3 ganglioside accumulation is visualized in grey matter throughout the brains of MPS I animals, including in the dentate gyrus and septal nucleus

(shown). This pattern of staining is absent in the brains of wild type animals and MPS I animals treated with AAV8-MCI. Scale bars are 100μm in length.

Author Manuscript Author Manuscript Author Manuscript Author Manuscript

Author Manuscript Author Manuscript Author Manuscript Author Manuscript

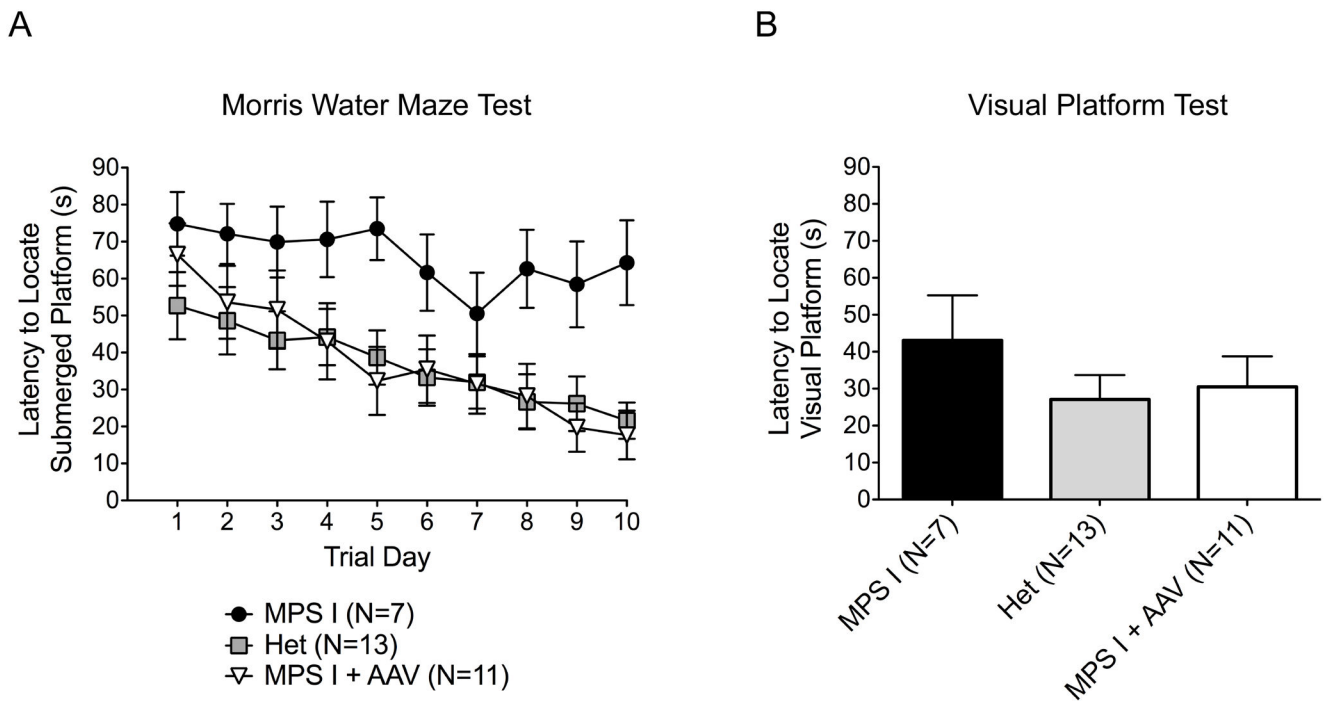

Figure 6.

A spatial learning and memory phenotype displayed by MPS I mice is completely prevented in MPS I mice treated by ICV infusion of AAV8-MCI as neonates. ***A***, Results of a modified Morris water maze task. MPS I mice displayed a significant deficit in their ability to locate a submerged platform compared to unaffected heterozygous mice (***P* = 0.001). MPS I mice treated with AAV8-MCI performed equivalent to heterozygous mice (***P* = 0.005 vs. MPS I mice). ***B,*** To confirm that the deficit displayed by MPS I mice was not due to impaired vision caused by corneal clouding or to musculoskeletal or cardiopulmonary abnormalities, the mice were subjected to a visual platform test. No significant difference was observed in this task between any of the groups of animals.